ISBN: 978-3-95450-214-1 ISSN: 2673-5490 doi:10.18429/JACoW-IPAC2021-WEPAB020

THE RELATION BETWEEN FIELD FLATNESS AND THE PASSBAND FREQUENCY IN THE ELLIPTICAL CAVITIES

G. T. Park, R. Rimmer, H. Wang
Thomas Jefferson National Laboratory, Newport News, VA, USA

Abstract

In SRF accelerator development, a technique that predicts the field flatness of the accelerating mode based on the passband frequency is highly desirable when the direct measurement of the field is not available. Such a technique is developed here for the SNS-PPU 6-cell SRF cavity whose field flatness is important for an efficient acceleration of the beam.

INTRODUCTION

A superconducting multi-cell elliptical cavity is now a standard technology for particle acceleration with its ultra-high quality factor Q_0 and the excellent accelerating gradient E_{acc}. Nevertheless, an accelerating gradient E_{acc} associated with the accelerating π mode as predicted from the bead-pull test [1] is not in general the same as the actual value in the operation with the beam. The E_{acc} is dependent on the field flatness, which may change significantly after the measurements either by surface treatment, mechanical stress applied afterwards or tuner action. This motivated the study on how to obtain the field flatness solely from the measurement of the passband frequencies without having to break vacuum for another bead-pull test. In the context of similar study on the three and half cell SRF-GUN cavity at Rossendorf, a numerical method that uses the solutions of the non-linear eigenvalue equations, which naturally arises in the equivalent circuit description of the cavity, was developed and successfully predicted the field flatness measurement [2]. In this paper, we extend the method to a six-cell elliptical cavity in the context of the performance verification of the SNS-PPU cavity from the Spallation Neutron Source (SNS), whose geometry is shown in Fig. 1. In principle, this method can be extended to a 9-cell cavity straightforwardly if numerical solutions to the corresponding eigenvalue equations are reliably obtained.

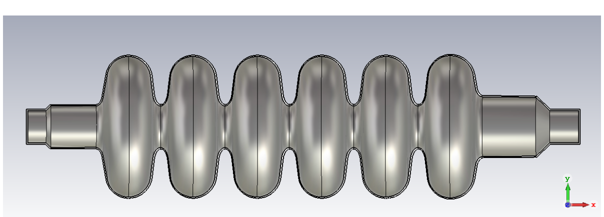

Figure 1: The SNS-PPU 6-cell elliptical cavity.

ANALYTICAL DESCRIPTION

A 6-cell cavity with loss can be described to a good approximation by an equivalent *RLC* circuit as shown in Fig. 2 [3].

Application of Kirchhoff's law to each cell of the circuit leads to the 6×6 matrix equation

$$\mathbf{A}V = \mathbf{B}V, \tag{1}$$

$$\text{where } \left[\mathbf{A}\right]_{nm} = (-k_{n,m+1})\delta_{n,m+1} + (-k_{n,m})\delta_{n,m-1} + (1 + k_{n,m} + k_{n,m+1})\delta_{n,m}, \tag{2}$$

$$\left[\mathbf{B}\right]_{nm} = \frac{\omega^2}{\omega_{0,n}^2}\left(1 - i\frac{1}{2Q_{0,n}}\right)\delta_{n,m}, \tag{3}$$

$$k_{nm} = \frac{C_n}{S_m}, \quad \omega_{0,n} = \frac{1}{\sqrt{L_n C_n}}, \quad Q_{0,n} = \frac{\omega}{2}\frac{L_n}{R_n}. \tag{4}$$

Here V is a column vector whose n-th component corresponds to the current in the n-th cell of the cavity and ω is a member of loaded passband (angular) frequency—complex number whose imaginary part corresponds to the decay constant of the mode. S_m is shunt capacitances between $(m-1)$-th and m-th cell. With an ideal cavity as designed—unlike the SRF-GUN cavity, the SNS-PPU is a TESLA type cavity with each cell identical in shape except for the end cells—, the circuit elements are all uniform , i.e., $L_1 = \cdots = L_6 \equiv L$, $C_1 = \cdots = C_6 \equiv C$, $R_1 = \cdots R_6 \equiv R$, $S_2 = \cdots = S_6 \equiv C_k$, $S_1 = S_7 = C_b$. This will naturally introduce "degeneracy" of the passband frequency in regards to deformed geometry and the field profiles. With the uniform elements, Eqs. (1), (3) and (4) reduce to

$$\mathbf{A}V = \lambda V, \tag{5}$$

$$\text{where } \lambda = \frac{\omega^2}{\omega_0^2}\left(1 - i\frac{1}{2Q_0}\right), \tag{6}$$

$$k = \frac{C}{C_k}, \quad \gamma = \frac{C_b}{C_k}, \quad \omega_0 = \frac{1}{\sqrt{LC}}, \quad Q_0 = \frac{\omega}{2}\frac{L}{R}. \tag{7}$$

Notice now V and λ appear as an eigenvector and eigenvalue of $\mathbf{A}$, called a circuit matrix, respectively. In general, 6×6 matrix $\mathbf{A}$ has six eigenvalues (and six corresponding eigenvectors) and the corresponding frequencies form a passband, which can be labeled as $\omega_1, \cdots \omega_6$ (the current amplitudes are similarly labeled as $V_1, \cdots V_6$). If λ_k's are real, ω_k's are complex numbers as the solutions to Eq. (6) with its imaginary part identified with the decay constant of the cavity. With a lossless cavity, $R = 0$, $Q_0 \to \infty$ and Eq. (6) reduces to $\lambda = \omega^2/\omega_0^2$.

Conversely, if a complete set of the field profiles V_k's and passband frequencies ω_k's are known, then one can construct a circuit matrix using eigenvalue decomposition theorem.

$$\mathbf{A} = \mathbf{J}\mathbf{D}\mathbf{J}^{-1}, \tag{8}$$

$$\text{where} \quad \left[\mathbf{J}\right]_{nm} = V_m^{(n)}, \quad \left[\mathbf{D}\right]_{nm} = \lambda_n \delta_{nm}, \tag{9}$$

ISBN: 978-3-95450-214-1 ISSN: 2673-5490 doi:10.18429/JACoW-IPAC2021-WEPAB020

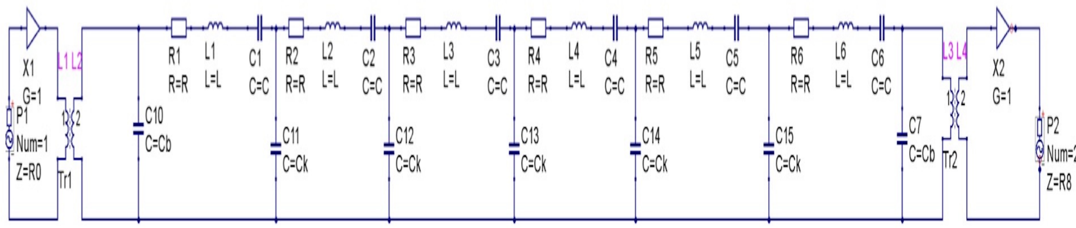

Figure 2: The equivalent circuit of the 6-cell SNS-PPU cavity. C_k is shunt capacitance between the cells—C_b is capacitance associated with the left/right beam pipe.

where $V_m^{(n)}$ refers to current amplitude of m-th mode in n-th cell. In general, the matrix $\mathbf{A}$ is not in a "canonical" form, i.e., with all the far-off diagonal elements being zero, nor symmetric.

Subsequently, the small deformation of the cavity geometry can be identified as the changes in the RLC circuit elements such as L, C, C_k, C_b and correspondingly the changed circuit matrix $\mathbf{A}'$ will have different eigenvectors and eigenvealues in Eq. (5), denoted as V', λ', respectively. Conversely, with the passband frequency known, one can find a small change $\mathbf{E} = \mathbf{A}' - \mathbf{A}$ in a circuit matrix such that

$$det\left\{\mathbf{A}' - \lambda'\mathbf{1}\right\} = det\left\{(\mathbf{A} + \mathbf{E}) - \lambda'\mathbf{1}\right\} = 0, \qquad (10)$$

which is a coupled system of 6 non-linear equations for $\mathbf{E}$ and can be numerically solved via various computation programs—we used the Matlab and the MathCAD solve block. In general, the elements in $\mathbf{E}$ are not uniquely determined by non-linear equations in Eq. (10), which would physically correspond to the fact that fields with many different profiles (stemming from different geometrical deformations) can have the same passband frequencies. For instance, in view of Eq. (10), any deformed geometry will have the same passband frequency as its mirror-reflection with respect to the center plane. In case of a SRF-GUN at Rossendorf, with non-identical baseline cell-geometry, Eq. (10) led to a unique solution for a small deformation. Once all the elements in $\mathbf{E}$ are known, then field profiles and flatness are obtained straightforwardly as eigenvectors and their peak values.

THE APPLICATIONS TO SIMULATIONS AND MEASUREMENTS

In this section, we check the validity of the methods developed in the previous section to predict the field profiles —field flatness of the π-mode, in particular—of the SNS-PPU cavities subject to various deformations. First, one computes $\mathbf{A}$ in Eq. (5) from the passband frequency and a complete set of the field profiles of "the reference cavity" obtained either from the simulations. Next we turn to the deformed cavity. The λ''s in Eq. (10) is computed from the measured passband frequency of the deformed cavity. Then the field profiles of a deformed cavity are predicted from the eigenvector of $\mathbf{A}'$ via Eq. (10). We use an undeformed cavity —designed to have the field flatness of ≥ 99 %—as our reference cavity to determine the mid-cell resonant (angular) frequency ω_0 (also k) so that the analytical formula Eq. (11) for the eigenvalues fits the given f_m's for all $m = 1, \cdots, 6$:

$$\lambda^{(m)} = \left(\frac{f_m}{f_0}\right)^2 = 1 + 2k\left[1 - \cos\left(\frac{m\pi}{N}\right)\right], \qquad (11)$$

where $N = 6$ is the number of the cells.

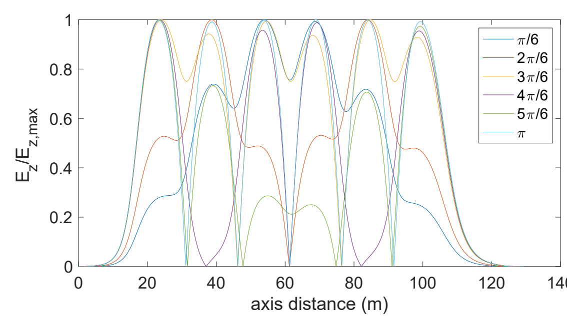

Figure 3: The field profiles of the reference cavity (from the Superfish simulation).

The "eigendata", i.e., a set of eigenvalues and eigenvectors was obtained from the simulations using the two FEA (Finite Element Analysis) codes, i.e., Superfish [4] and the CST-MWS [5]—the frequencies and field profiles are almost identical between the Superfish and the CST. The passband frequencies are summarized in Table 1 and the field profiles in Fig. 3 and Table 2. Subsequently, f_0 is determined to be $f_0 = 792.820$ MHz.

Therefore, one can compute $\mathbf{A}$ as

$$\begin{bmatrix} 1.023 & -0.008 & 0 & 0 & 0 & 0 \\ -0.008 & 1.015 & -0.008 & 0 & 0 & 0 \\ 0 & -0.008 & 1.015 & -0.008 & 0 & 0 \\ 0 & 0 & -0.008 & 1.015 & -0.008 & 0 \\ 0 & 0 & 0 & -0.008 & 1.015 & -0.008 \\ 0 & 0 & 0 & 0 & -0.008 & 1.023 \end{bmatrix},$$

which is approximately symmetric.

Further inspections into the elements of $\mathbf{A}$ confirms that $k = 0.008$ and consistent with the circuit theory prediction in Eq. (2).

Now consider the deformed cavity geometries. The associated eigendata was obtained from the measurements made

ISBN: 978-3-95450-214-1 ISSN: 2673-5490 doi:10.18429/JACoW-IPAC2021-WEPAB020

Table 1: The Passband Frequencies of the Reference and Deformed SNS-PPU Cavity

Passband	Superfish	CST	Vendor	Jlab
$\pi/6$	793.625	793.611	792.513	792.739
$2\pi/6$	795.858	795.843	794.759	795.015
$3\pi/6$	798.896	798.880	797.916	798.126
$4\pi/6$	801.919	801.902	801.087	801.250
$5\pi/6$	804.122	804.104	803.286	803.468
π	804.938	804.920	804.124	804.288

Table 2: The Field Profile Matrix **J** of the Reference SNS-PPU Cavity. The E-field Amplitudes of the Passband Modes Were Taken at the Geometrical Center of Each Cell In Fig. 3

Modes	$\pi/6$	$2\pi/6$	$3\pi/6$	$4\pi/6$	$5\pi/6$	π
cell 1	0.28	0.53	1.00	1.00	1.00	-1.00
cell 2	0.74	1.00	0.94	0.00	-0.73	0.99
cell 3	1.00	0.49	-0.99	-0.96	0.29	-1.00
cell 4	0.99	-0.53	-0.94	0.99	0.25	1.00
cell 5	0.72	-1.00	1.00	0.00	-0.71	-1.00
cell 6	0.25	-0.48	0.93	-0.95	0.97	0.99

at the Vendor (Research Instrument in Germany)—with flat π-mode—and the Jefferson Lab.

As stated previously, we use the passband frequencies to predict the field profiles, which will be compared with those from the eigendata. First we start with the Vendor measurement whose $f_{0,V}$ can also be determined to be $f_{0,V} = 791.65$ MHz via Eq. (11). The circuit matrix deformation **E** is obtained by solving Eq. (10) with **E** constrained to be near $e_0 \sim 10^{-3}$:

$$\mathbf{E} = 10^{-4} \times \begin{bmatrix} 7.9 & -1.6 & 0.3 & 1.3 & 0.9 & 0.4 \\ -1.8 & 4.4 & -2.3 & 0.2 & 0.4 & 0.9 \\ 0.2 & -2.3 & 4.3 & -3.2 & 0.2 & 0.1 \\ 1.3 & 0.3 & -3.1 & 4.4 & -2.3 & 0.3 \\ 0.8 & 0.3 & 0.3 & -2.3 & 4.4 & -1.6 \\ 0.3 & 0.8 & 1.2 & 0.2 & -1.7 & 8.0 \end{bmatrix}.$$

We have not understood the significant presence of the far-off diagonal elements in Eq. (12)—when solved with **E** constrained to have zero far-off diagonals, the solution was unphysical. The expected corresponding field profiles of $\mathbf{A}'$ is given as

$$\mathbf{J}' = \begin{bmatrix} 0.26 & -0.53 & 0.98 & -1.00 & 1.00 & 1.00 \\ 0.73 & -1.00 & 0.94 & 0.00 & -0.72 & -0.99 \\ 1.00 & -0.49 & -0.96 & 0.96 & 0.29 & 1.00 \\ 0.99 & 0.53 & -0.90 & -0.99 & 0.25 & -1.00 \\ 0.70 & 1.00 & 1.00 & 0.00 & -0.70 & 1.00 \\ 0.24 & 0.48 & 0.91 & 0.96 & 0.97 & -0.99 \end{bmatrix},$$

which gives a good agreement (within 1%) with the Vendor measurement for the π mode in Table 3.

Next, the measurement at the Jefferson Laboratory is not with flat π-mode. If the deformation is limited only to the

Table 3: The Field Profiles of the Deformed SNS-PPU Cavity in Two Measurements

	Jlab						Vendor
Cell	$\pi/6$	$2\pi/6$	$3\pi/6$	$4\pi/6$	$5\pi/6$	π	π
cell 1	0.35	0.56	1.00	1.00	1.00	-0.93	-1.00
cell 2	0.81	1.00	0.92	0.09	-0.74	0.94	0.98
cell 3	1.00	0.42	-0.94	-0.91	0.31	-0.98	-1.00
cell 4	0.95	-0.20	-0.87	0.95	0.22	0.97	1.00
cell 5	0.73	-0.90	0.96	0.08	-0.66	-0.96	-0.99
cell 6	0.27	-0.35	0.74	-0.87	0.94	1.00	0.99

C_k's, Eq. (7) would suggest f_0 remains the same as the undeformed cavity and we again solve Eq. (10) near $e_0 \sim 2\times10^{-3}$ to have

$$\mathbf{E}_{Jlab} = 10^{-3} \times \begin{bmatrix} 1.9 & 0.7 & 1.7 & 2.7 & 2.7 & 1.7 \\ 0.5 & -0.2 & 1.0 & 3.0 & 2.7 & 2.7 \\ 1.6 & 0.9 & 1.5 & 1.3 & 3.0 & 2.7 \\ 2.7 & 3.1 & 1.2 & 1.5 & 1.0 & 1.7 \\ 2.7 & 2.6 & 3.1 & 0.8 & -0.2 & 0.7 \\ 1.6 & 2.7 & 2.7 & 1.7 & 0.5 & 2.0 \end{bmatrix},$$

$$\mathbf{J}_{Jlab} = \begin{bmatrix} -0.16 & 0.52 & 0.55 & 1.00 & 1.00 & -0.94 \\ 0.33 & 1.00 & 0.96 & 0.02 & -0.48 & 0.95 \\ 1.00 & 0.49 & -0.26 & -0.96 & 0.35 & -0.96 \\ 1.00 & -0.52 & -0.21 & 1.00 & 0.26 & 0.98 \\ 0.32 & -1.00 & 1.00 & 0.02 & -0.40 & -0.99 \\ -0.16 & -0.48 & 0.49 & -0.97 & 0.93 & 1.00 \end{bmatrix}.$$

Eq. (12) agrees reasonably with those in Table 3 on π mode, although some low-lying modes have poorer agreements. The discrepancy suggests the deformation is not limited to C_k's but extends over to L, C's, changing ω_0. Moreover, according to on-going study based on a series of the CST simulations, the current algorithm accurately predict the field flatness corresponding to $|\mathbf{E}| \lesssim 5\times10^{-3}$, beyond which the field profiles start to deform significantly. These issues would require a deeper study with more measurement data.

CONCLUSION

The technique that can predict the field profiles of the 6-cell SNS-PPU cavity based solely on the measurements of the passband frequency is proven to be effective.

REFERENCES

[1] A. Sun, H. Wang, and G. Wu, “Effect of the Tuner on the Field Flatness of SNS Superconducting RF Cavities”, in *Proc. 22nd Linear Accelerator Conf. (LINAC’04)*, Lübeck, Germany, Aug. 2004, paper THP92, pp. 815–817.

[2] A. Arnold, H. Buettig, D. Janssen, G. Staats, and J. Teichert, “Field reconstruction by passband frequency measurement at the Rossendorf SRF-gun cavity”, in *Proc. 13th Int. Conf. RF Superconductivity (SRF’07)*, Beijing, China, Oct. 2007, paper WEP77, pp. 689–691.

ISBN: 978-3-95450-214-1 ISSN: 2673-5490 doi:10.18429/JACoW-IPAC2021-WEPAB020

[3] H. Padamsee, J. Knobloch, and T. Hayes, *RF Superconductivity for Accelerators 2nd edition*. New Jersey, United States: Wiley-VCH, 2007.

[4] Poisson Superfish, https://laacg.lanl.gov/laacg/services/download_sf.phtml

[5] CST, http://www.cst.com